Journal of Thermal Analysis and Calorimetry, Vol. 62 (2000) 111–122

TRANSITION STATE OF HEAT DENATURATION OF METHIONINE AMINOPEPTIDASE FROM A HYPERTHERMOPHILE

S. A. Potekhin[1], *K. Ogasahara*[2] *and K.Yutani*[2]

[1]Institute of Protein Research, Russian Academy of Sciences, 142292 Pushchino, Moscow Region Russia
[2]Institute for Protein Research, Osaka University, Yamadaoka, Suita, Osaka 565, Japan

Abstract

Heat denaturation of methionine aminopeptidase from a hyperthermophile *Pyrococcus furiosus* (*Pf*MAP) was studied by differential scanning calorimetry at acid pH. Analysis of the calorimetric data has shown that denaturation of *Pf*MAP is non-equilibrium at heating rates from 0.125 to 2 K min^{-1}. This means that the protein structure at these conditions is metastable and its stability (the apparent temperature of denaturation T_m) is under kinetic control. It was shown that heat denaturation of this protein is a one-step kinetic process. The enthalpy of the process and its activation energy were measured as functions of temperature. The obtained data allowed us to estimate the heat capacity increment and the change in the number of bound protons during activation of the molecule. The data also suggest that the conformation of *Pf*MAP at the transition state only slightly differs from its native conformation with respect to compactness, hydration extent and hydroxyl protonation.

Keywords: calorimetry, kinetic model, *Pf*MAP, transition state

Introduction

Specific features of proteins from hyperthermophiles are their increased thermal stability and an extremely low level of structure motility. There are numerous publications aimed at clarifying physical reasons for increased thermal stability which is important for understanding the nature of forces stabilizing protein structure. Herein the structure stability is taken to be the temperature of the middle of the denaturation transition T_m under given conditions.

It is known that thermal stability of proteins can be of different origin. When it is thermodynamic stability, the ratio of populations of the native N and denatured D states is determined by the equilibrium constant K=[D]/[N] and does not depend on time. In its turn, the equilibrium constant is determined by the free energy of structure stabilization, i.e. by the difference of the free energy values for the denatured and native states. Therefore, the melting curves are equilibrium and described by the van't Hoff model [1, 2] or the model of equilibrium multistage denaturation [2–5].

1418–2874/2000/ $ 5.00

Akadémiai Kiadó, Budapest
Kluwer Academic Publishers, Dordrecht

The protein structure can also be metastable. The protein can remain native even at a rather high temperature when this state is not favorable from the thermodynamic point of view. Such behavior is explained by a very slow rate of denaturation at the temperature region where the denatured state becomes thermodynamically favorable. Denaturation may last for many hours and even days under this condition [6–9]. Correspondingly DSC transitions must be analyzed on the basis of kinetic terms [10–14]. In this case, the main factor that determines the macromolecule stability is the magnitude of the energetic barrier between the native and denatured states and its dependence on temperature. By definition, the transition state is the most unfavorable energetically. This state is virtual. The life time and population of this state is very low under any conditions. Thus, it is practically impossible to study structural peculiarities of this state in equilibrium or kinetic experiments by direct methods. Thus, the only way to obtain any information about transition state is to keep track of constant rate and activation energy dependence on conditions and protein structure. Then we can use our knowledge about the correlation between structural and energetic parameters to clarify some structural features of the transition state. Specific features of the transition state were studied upon denaturation of several proteins [15–19], however there are no data yet suggesting the existence of any structural peculiarities of this state of hyperthermophilic proteins.

Scanning microcalorimetry is one of the most convenient methods for studying heat denaturation of proteins and for obtaining thermodynamic characteristics of the process. A mathermatical apparatus has been suggested to carry out thermodynamic analyses of calorimetric curves and to reveal thermodynamically stable states of macromolecules that are realized at increased temperatures [2–5]. However, the thermodynamic analysis of calorimetric curves requires the denaturation process to proceed at equilibrium conditions, which does not always take place. In many cases heat denaturation of proteins is a kinetically driven process. As a result, such thermodynamic functions of structure stabilization as entropy and Gibbs free energy cannot be obtained from microcalorimetric curves. Nevertheless, in these cases the shape of melting curves can provide very useful information about kinetic parameters of denaturation [10–13].

The aim of this paper is to investigate thermal denaturation of MAP from hyperthermophiles using scanning microcalorimetry and to clarify main thermodynamic and kinetic parameters of the process.

Materials and methods

*Pf*MAP was expressed in *E. Coli* and purified as described [20]. The protein concentration was estimated from the maximum absorbance at the wavelength of 278.5 nm, using $E^{1\%}$=9.63 with a cell of 1-cm light path length. This value was determined based on the protein assay by the Lowry method using bovine serum albumin as a standard protein.

Calorimetric measurements were made on a precision scanning microcalorimeter DASM-4A (‘Biopribor’, Pushchino), with platinum cells of 0.5 ml volume at

scanning rates 1.0 K min^{-1} and excess pressure of 2.2 kg cm^{-2}. The protein concentration in the experiments varied from 0.7 to 1.4 mg ml^{-1}. The experiments were performed in 25 mM glycine–HCl solution at pH 2.8–3.9. Prior to the measurements, *Pf*MAP solution was dialyzed overnight *vs*. a buffer solution at 4°C. In all cases, Co^{2+} was not present in the buffer solutions. Both dialyzed samples and the last dialysis buffer were filtered through a 0.22 mm pore size filter and then degassed in vacuum. The partial specific volume was accepted to be 0.73 cm^3 g^{-1}. The excess partial heat capacity was calculated in a standard manner [2]. Experiments at different heating rates (0.5, 1 and 2 K min^{-1}) were carried out with a model 5100 Nano-DSC (Calorimetry Sciences Corp.) with the pressure of 2.9 kg cm^{-2} in the cells.

The activation energy of denaturation at T_m was calculated by fitting the experimental curves with the model one. It is known [8, 12] that the shape of a heat absorption curve for an irreversible one-stage process is described as

$$c_{p,exc} = ec_p^{max} \exp\left[\frac{\Delta E_{uf}(T-T_m)}{RT_m^2}\right] \exp\left\{\exp\left[\frac{\Delta E_{uf}(T-T_m)}{RT_m^2}\right]\right\} \quad (1)$$

where T_m is the apparent temperature of denaturation, ΔE_{uf} is the activation energy, c_p^{max} is the excessive heat capacity at the trace maximum, T is the absolute temperature, R is the gas constant and e stands for the natural logarithm base. The function depends on three parameters: T_m, c_p^{max} and ΔE_{uf}. In general, these parameters are not independent and are coupled by the ratio [10, 21]

$$\Delta E_{uf} = \frac{eRT_m^2 c_p^{max}}{\Delta H_m} \quad (2)$$

where ΔH_m is the melting enthalpy.The rate constant of denaturation at T_m, $k_{uf}(T_m)$ can be readily estimated by formula (3) using the calculated parameters

$$k_{uf}(T_m) = \frac{\Delta E_{uf} V}{RT_m^2} \quad (3)$$

The constant rate of unfolding k_{uf} obtained from these experiments was extrapolated to any temperature using its temperature dependence. The temperature dependence of this parameter is described by the transition-state theory:

$$k_{uf}(\mathrm{pH},T) = \frac{k_B T}{h} \exp\left[-\frac{\Delta G_{uf}^{\#}(\mathrm{pH},T)}{RT}\right] \quad (4)$$

where k_B is Boltzmann's constant, h is Plank's constant and $\Delta G_{uf}^{\#}(\mathrm{pH},T)$ is activation free energy, which is here the difference in the Gibbs free energy between the native state and the transition state of unfolding. Using the thermodynamic identity

$$\Delta G_{uf}^{\#}(\mathrm{pH},T) = \Delta H_{uf}^{\#}(T) - T\Delta S_{uf}^{\#}(\mathrm{pH},T) \quad (5)$$

where $\Delta H^{\#}_{uf}(T)$ is the activation enthalpy and $\Delta S^{\#}_{uf}(\mathrm{pH},T)$ is the activation entropy, and taking into consideration those temperature dependences of these function can be written as

$$\Delta H^{\#}_{uf}(T)=\Delta H^{\#}_{uf}(T_m)+\Delta C^{\#}_{p,uf}(T-T_m) \quad (6)$$

$$\Delta S^{\#}_{uf}(\mathrm{pH},T)=\Delta S^{\#}_{uf}(\mathrm{pH},T_m)+\Delta C^{\#}_{p,uf}\ln\left(\frac{T}{T_m}\right) \quad (7)$$

the constant rate of unfolding k_{uf} can be evaluated at any temperature. On the basis of the transition-state theory we assume that the Arrhenius activation energy ΔE_{uf} is approximately equal to the enthalpy of the transition state.

Results

Figure 1 shows the temperature dependence of the partial molar heat capacity for MAP at pH from 2.8 to 3.8. As described [20], when pH drops below 2.8, the denaturation peak on heat absorption curves disappears. The last heat absorption peak is observed at about 70°C. A specific feature of the obtained curves is the asymmetry of excess heat absorption peaks. There may be two reasons for this: (1) the denaturation is a multi-stage process, and/or (2) the observed transition has a kinetic character, i.e. it is non-equilibrium. This is reasonable since repeated heating of the samples revealed almost complete irreproducibility of denaturation curves upon recurrent heating. However, the irreproducibility established in such a way is not always pure thermodynamic irreversibility [2, 22] and may be caused by slow processes following equilibrium denaturation, e.g. slow chemical modifications or aggregation. In such cases the shape of melting curves is not practically distorted and can be treated by using equilibrium thermodynamics. Therefore, before using any model for analysis, denaturation and respective calorimetric profiles should be studied in detail.

To verify whether the denaturation process is equilibrium, melting curves have been obtained at different heating rates. Figure 2 shows that they have a noticeable shift in temperature depending on the heating rate, which evidences non-equilibrium conditions of the experiment. This means that denaturation under the given conditions is either thermodynamically irreversible or the heating rates are too high to consider this process as equilibrium. It was shown earlier [11, 14, 23] that in both cases the melting curve has a similar shape. Indeed, even when protein denaturation is reversible and proceeds in one stage, but the heating rates significantly exceed the value

$$V_{max}=\frac{RT_d^2}{\Delta H_m \tau_d} \quad (8)$$

where T_d is the real (equilibrium) temperature of denaturation, $\tau_d=(k_{uf}+k_r)^{-1}$ is the relaxation time, the melting curves would be well described by the irreversible kinetic scheme:

$$N \xrightarrow{k} D \quad (9)$$

In other words, if the denaturation rate at T_d is low enough, denaturation proceeds in a non-equilibrium way and the curve shape is indistinguishable from that of an irreversible process.

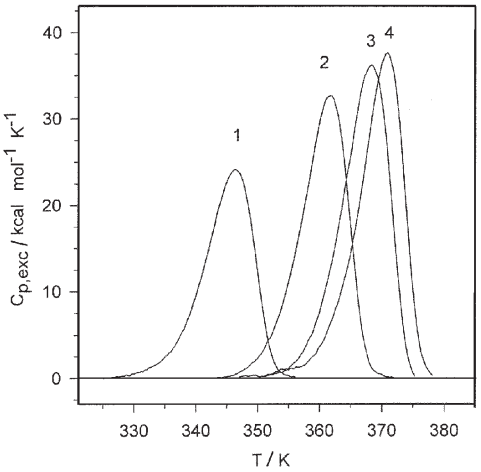

Fig. 1 Dependence of the excess partial heat capacity of MAP on temperature at different pH. Curves 1–4 correspond to pH 2.83, 3.35, 3.58 and 3.72, respectively. The curves were obtained at 1 K min^{-1}

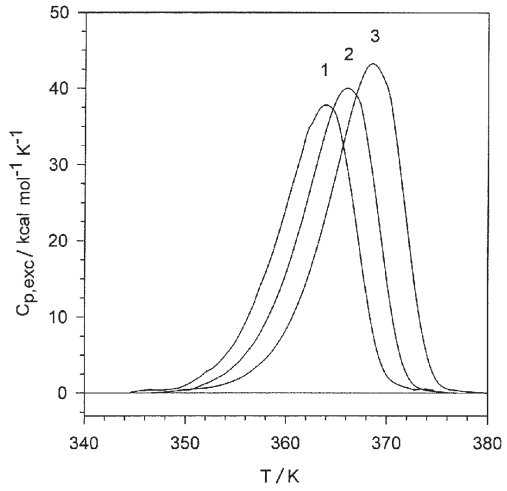

Fig. 2 Dependence of the excess partial heat capacity of MAP on temperature at pH 3.46 and different heating rates: (1) 0.5, (2) 1.0, (3) 2.0

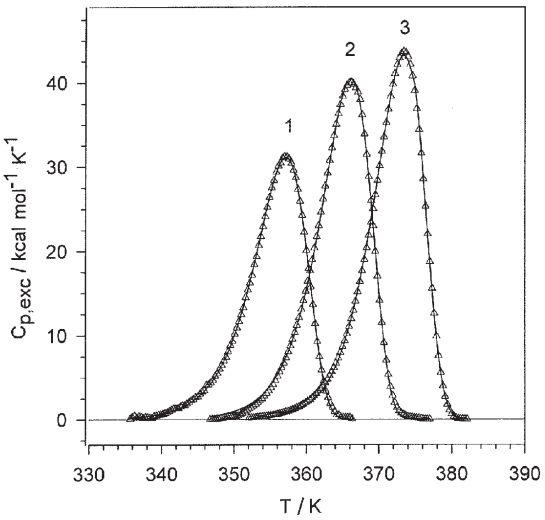

Fig. 3 Best fit of the experimental excess heat capacity functions of MAP (Δ) using a one-stage kinetic model. (1) pH 3.23, V=0.5 K min^{-1}; (2) pH 3.46, V=1.0 K min^{-1}; (3) pH 3.78, V=2 K min^{-1}. Experimental curves are shown by solid lines

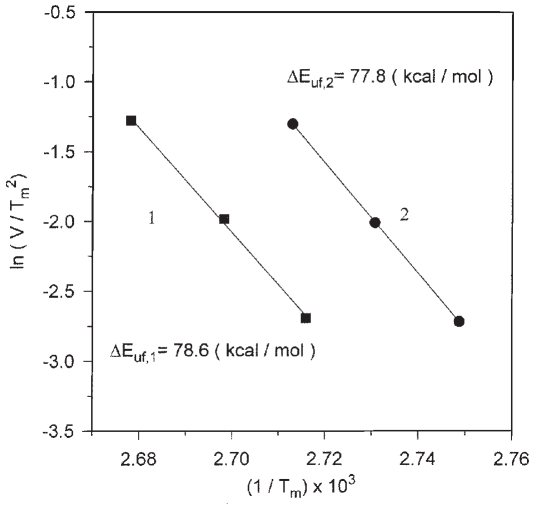

Fig. 4 Dependence of ln(V/T_m^2) *vs.* the reciprocal apparent denaturation temperature $1/T_m$. Experimental points were obtained at heating rates (V) 2.0, 1.0, 0.5 K min^{-1}. Lines show best fit by linear functions. Experimental points were obtained at pH 3.78 (1) and pH 3.46 (2)

The other problem that should be clarified is the number of stages in the given kinetic process (the number of states realized upon increasing the temperature).

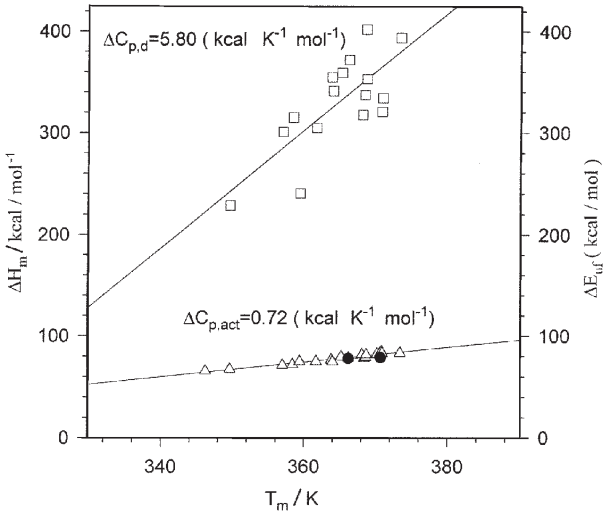

Fig. 5 Dependence of enthalpy (squares) and activation energy (triangles) for denaturation *vs.* the apparent denaturation temperature T_m. The activation energy obtained from experiments on the dependence of the apparent melting temperature on the heating rate (Fig. 4) is shown by filled circles. Straight lines are drawn by the least-squares method and correspond to heat capacity increments given in the figure

Using the least-squares method we determined the parameters corresponding to the best description of experimental curves by a one-step kinetic formalism, as described in Materials and methods. Initial values for the activation energy were evaluated by formula (2). Figure 3 shows examples of such a description. As seen from the figure, excess heat absorption curves are well compatible with this one-step model. Figure 5 presents denaturation enthalpy and activation energy calculated from the experimental curves.

One more circumstance should be taken into account. Activation energy values can be estimated in two ways: either from the shape of the curves as it was demonstrated earlier, or from the dependence of the apparent denaturation temperature T_m on the heating rate [11, 21]. Figure 4 gives this dependence. The function is linear which suggests non-equilibrium melting even at the minimal heating rate studied. The activation energy values calculated from this dependence and directly from the shape of the curves (Fig. 5) are well compatible. This fact additionally corroborates the correspondence of the experimental data to the model used.

Figure 5 shows the dependence of the activation energy of denaturation. On the basis of the transition-state theory the activation energy is approximately equal to the enthalpy of the transition state. The function is linear and increases slightly with a temperature increase. The dependence of the denaturation enthalpy is also given there. It is known that the denaturation enthalpy of proteins is practically independent of solution pH [1] and is a function of temperature only. Abnormal titration of groups

that can occur upon denaturation does not contribute noticeably to the denaturation enthalpy at least at acid pH. The same assumption may be also taken for the activation energy [7, 15, 24]. This means that the slope of the dependencies given in Fig. 5 should coincide with the corresponding heat capacity increments. Their values are 5.8 and 0.72 kcal mol^{-1} K^{-1} for denaturation and activation, respectively, i. e. during transition to the activated state the change of the toxin heat capacity does not exceed 13% of the heat capacity increment for denaturation.

Discussion

The denaturation process for *Pf*MAP is well compatible with the irreversible one-stage model. Consequently, heat denaturation is non-equilibrium and proteins have no intermediate states at experimental heating rates. Howeve, it does not mean that the denaturation is inevitably thermodynamically irreversible and the native state of the protein is not favorable energetically through the temperature range. The reason may be a slow rate of denaturation at the real transition temperature T_d [11, 14, 23]. In any case, an important result of this work is that the structure of MAP in the native state is maintained due to a high activation barrier rather than thermodynamic expedience of this state, at least at high-temperatures. However, the native state may be energetically favorable at sufficiently low-temperatures since the protein structure is completely restored after the removal of the urea. On the other hand, we have already shown [23] that irreproducibility of the curves at repeated heating (apparent irreversibility) can be caused by a low rate of folding at decreased temperatures when the native state becomes at last energetically expedient.

Taking into account that denaturation of *Pf*MAP has a non-equilibrium character, it is possible to determine only two thermodynamic parameters for this process. They are the heat capacity increment and the denaturation enthalpy (Fig. 5). For the given protein, these parameters are within a standard range of values for globular proteins [1]. There are no grounds to suggest that these parameters for proteins from hyperthermophiles differ significantly from those for proteins from usual bacteria. Non-equilibrium of denaturation does not permit to obtain real temperature of denaturation T_d and, consequently, the change of the entropy and Gibbs free energy.

Several conclusions can be drawn on the structure of the transition state for *Pf*MAP. As seen from Fig. 5, the heat capacity increment for the transition state is significantly lower than the heat capacity increment for denaturation. It is consistent with the results demonstrated earlier for lysozyme [15], barnase [17], cold-shock protein CspB [18], δ-endotoxin [19], but not for chymotrypsin inhibitor 2. In the latter case, the increment of heat capacity for the transition state is intermediate between the native and denatured conformations [16]. Since the heat capacity increment correlates well with the hydrophobic surface exposure during conformational transition [1], it should be accepted that the transition state of *Pf*MAP is only slightly distinct from the native state in the exposure of hydrophobic groups and, hence, is as compact as the native one.

There is one more energy criterion frequently used to estimate compactness of globular proteins. As shown earlier [1, 26], the specific enthalpy of denaturation extrapolated to 100–110°C is the same for many compact globular proteins (13 cal g^{-1} K^{-1}). In this temperature range, the denaturation enthalpy for *Pf*MAP is 11.6–13.4 cal g^{-1} K^{-1}, which is close to the standard value. However, the specific enthalpy of the transition state (the specific enthalpy of activation) is much lower varying from 2.4–2.6 cal g^{-1} K^{-1}. As a rule, a decrease in enthalpy at this temperature is explained by disruption of Van der Waals contacts and hydrogen bonds [1]. Thus, according to this criterion the molecule structure has quite essential distortions, though no additional hydration of the surface of hydrophobic groups takes place. So, we have to accept that the energy barrier between native and denatured conformations is required for disruption of short-range interactions in a certain part of the molecule. Additionally, a large value of the activation energy strongly suggests that this disruption is of a collective origin.

Figure 5 shows that ΔE_{uf} is positive up to very low-temperatures. Hence, the rate of denaturation should increase when the temperature increases, because the derivative of the rate constant for any process with respect to the temperature is proportional to the activation energy of the process. The ratio of the denaturation enthalpy to the activation energy depends strongly on temperature. Taking into account that for one-step denaturation the enthalpy should be connected with the activation energies for direct and reverse processes

$$\Delta H_m = \Delta E_{uf} - \Delta E_f \tag{10}$$

the activation energy of renaturation can be readily calculated. It is clear that this value changes its sign in the temperature range from 310 to 320 K. Consequently, the rate of folding must reach its maximal value in this temperature range and decrease both with decreasing and increasing the temperature. Such a behavior of folding/unfolding rates is usual for proteins which is corroborated by direct measurements of the dependence of the rate of folding/unfolding on temperature [15, 18, 27].

The kinetic parameters obtained make it possible to estimate the constant of denaturation rate in a wide range of pH and temperature. Figures 6 and 7 show corresponding dependencies. It is seen that the denaturation rate slows down with a temperature decrease and pH increase, which is the reason for apparent stabilization (a shift of T_m to higher temperatures) for *Pf*MAP. Therefore it is evident that with a decrease of pH, the transition state is destabilized compared to the native one. In other words, protons bind predominantly with the transition state, which suggests different pK_a of a number of carboxyl groups titrated in this range of pH. Usually pK_a values of carboxyl groups are shifted due to electrostatic interactions and, in the first place, salt bridges. Thus it may be possible that notwithstanding that the protein remains rather compact in the transition state, some salt bridges in its structure are distorted. The number of groups, titrated additionally during MAP transition to the transition state, can be readily estimated by calculating the dependence of the free energy of activation on pH. Indeed, it is known that the difference in the number of bound protons be-

tween two protein conformations Δn is related to the pH dependence of free energy difference between these conformation ΔG [28, 29]:

$$\frac{\partial \Delta G}{\partial \mathrm{pH}} = 2.3RT\Delta n \tag{11}$$

This equation applies also to the unfolding rate constant but will, in this case, yield the change in ionization between the native state and the rate-limited transition state [25]. Figure 8 shows that the difference in the number of bound protons in the native and transition states grows from zero at pH above 3.7 to 5.3 at pH below 3.0. Thus no less than five carboxyl groups titrated abnormally change drastically their pK_a upon transition of the protein to the activated state. Unfortunately it is impossible to calculate Δn at lower pH, because the protein denatures in these conditions even at room temperature. However it seems probable that at such pH, Δn reaches its maximal value. Indeed, it is usually accepted that pK^{Asp}=3.9 and pK^{Glu}=4.1 [30], and the range of titration of the groups does not exceed ±1 unit of pH around its pK_a. This is demonstrated for barnase when Δn has its maximal value at pH about 3.0 [25]. Unfortunately, at present the absolute number of abnormally titrated groups in the native structure of *Pf*MAP is not known. This does not allow us to estimate what part of salt bridges is distorted upon transition to the activated state. However, it can be suggested that this part is not great. Indeed, nearly 96 ionic pairs with carboxyl groups at a distance of 6 Å have been revealed in the structure of *Pf*MAP [20]. Even if we take a ruder criterion, e.g. 3 Å, the number of such pairs will be at least 12. This allows us to

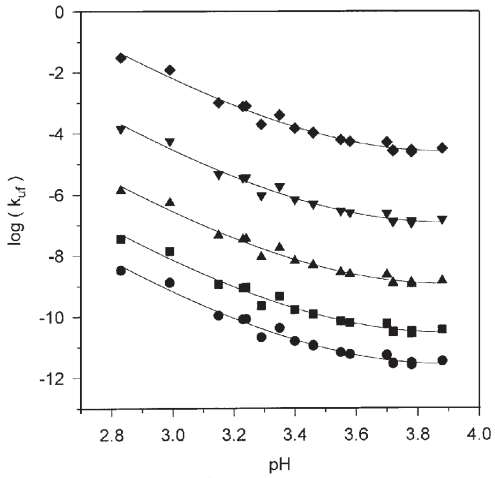

Fig. 6 Calculated dependence of the logarithm of the denaturation rate constant on pH at different temperatures. The points were calculated from the experimental data as described in Materials and methods. Continuous curves are the best approximation of this dependence with a quadratic parabola. Curves from top to bottom correspond to temperatures 353, 333, 313, 293 and 273 K, respectively

confirm that not every salt bridge is distorted during molecule transition to the activated state.

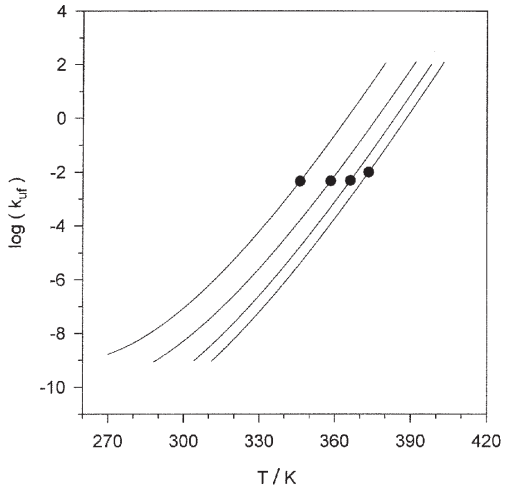

Fig. 7 Dependence of the logarithm of the denaturation rate constant on temperature at different pH. The curve is calculated from the experimental data as described in Materials and methods. Curves from right to the left correspond to pH 3.78, 3.46, 3.15 and 2.83. Symbols show results determined experimentally

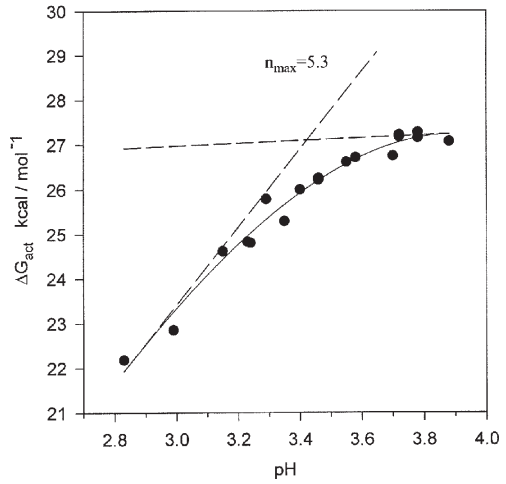

Fig. 8 Dependence of the free energy of activation on pH at 360 K. Points were calculated from the experimental data as described in Materials and methods. The dependence is approximated by the third-power polynomial (continuous line). Dashed lines show tangents to this curve corresponding to the minimal and maximal slopes

Thus, experimental observations of the unfolding kinetics by DSC suggest that the transition state of *Pf*MAP unfolding is a compact dehydrated conformation close to the native state. The data on the nature of the activated state of PfMAP are in good agreement with the results obtained earlier for barnase and other proteins, though MAP essentially exceeds them in size. Similar properties were also demonstrated for Cry3A δ-endotoxin, which is a large multidomain protein [19].

References

1 P. L. Privalov, Adv. Protein Chem., 33 (1979) 167.
2 P. L. Privalov and S. A. Potekhin, Methods in Enzymology, 131 (1986) 1.
3 E. Freire and R. L. Biltonen, Biopolymers, 17 (1978) 463.
4 P. L. Privalov, Adv. Protein Chem., 35 (1982) 1.
5 S.-J. Kidokoro and A. Wada, Biopolymers, 26 (1987) 213.
6 D. E. McRee, S. M. Redford, E. D. Getzoff, J. R. Lepock, R. A. Hallewell and J. A. Tainer, J. Biol. Chem., 265 (1990) 14234.
7 B. Chen and J. King, Biochemistry, 30 (1991) 6260.
8 F. Conejro-Lara, J. M. Sanchez-Ruiz, P. L. Mateo, F. J. Burgos, J. Vandrell and F. X. Aviles, Eur. J. Biochem., 200 (1991) 663.
9 M. L. Galisteo, P. L. Mateo and J. M. Sanchez-Ruiz, Biochemistry, 30 (1991) 2061.
10 E. Freire, W. W. van Osdol, O. L. Mayorga and J. M. Sanchez-Ruiz, Annu. Rev. Biophys. Chem., 19 (1990) 159.
11 J. R. Lepock, K. P. Ritchie, M. C. Kolios, A. M. Robahl, K. A. Heinz and J. Kruuv, Biochemistry, 31 (1992) 12706.
12 J. M. Sanchez-Ruiz, Biophys. J., 61 (1992) 921.
13 D. Milardi, C. La Rosa and D. Grasso, Biophys. Chem., 52 (1994) 183.
14 S. A. Potekhin and E. L. Kovrigin, Biofizika (Russia), 43 (1998) 223.
15 S. Segawa and M Sugihara, Biopolymers, 23 (1984) 2473.
16 S. F. Jackson and A. R. Fersht, Biochemistry, 30 (1991) 10428.
17 M. Oliveberg and A. R. Fersht, Biochemistry, 35 (1996) 2738.
18 T. Schindler and F. X. Schmid, Biochemistry, 35 (1996) 16833.
19 S. A. Potekhin, O. I. Loseva, E. I. Tiktopulo and A. P. Dobritsa, Biochemistry, 38 (1999) 4121.
20 K. Ogasahara, E. A. Lapshina, M. Sakai, Y. Izu, S. Tsunasawa, I. Kato and K. Yutani, Biochemistry, 37 (1998) 5939.
21 J. M. Sanchez-Ruiz, J. L Lopez-Lacomba, M. Cortijo and P. L. Mateo, Biochemistry, 27 (1988) 1648.
22 T. Vogl, C. Jatzke, H.-J. Hinz, J. Benz and R. Huber, Biochemistry, 36 (1997) 1657.
23 S. A. Potekhin and E. L. Kovrigin, Biophys. Chem., 73 (1998) 241.
24 B. Chen, W. Baase and J. A. Shellman, Biochemistry, 28 (1989) 691.
25 M. Oliveberg and A. R. Fersht, Biochemistry, 35 (1996) 2726.
26 P. L. Privalov and N. N. Khechinashvili, J. Mol. Biol., 86 (1974) 665.
27 Y.-J. Tan, M. Oliveberg and A. R. Fersht, J. Mol. Biol., 264 (1996) 377.
28 C. Tanford, Adv. Protein Chem., 24 (1970) 1.
29 C. Tanford, Adv. Protein Chem., 24 (1962) 69.
30 T. Creighton, Proteins, W. H. Freeman and Company, New York 1993.